

Supplementary Information for

Ionic-electronic transport interplay sustaining composition-tolerant terahertz absorption in organic mixed conductors

Wenbo Fan¹, Chaoyang Kuang^{2,3,*}, Yaokai Niu¹, Hongbo Wang⁴, Qiye Wen^{1,*},
Kai Xu^{4,*}, and Shangzhi Chen^{1,*}

¹ School of Electronic Science and Engineering, University of Electronic Science and Technology of China, Chengdu, 611731, China

² Laboratory of Organic Electronics (LOE), Department of Science and Technology (ITN), Linköping University, Campus Norrköping, Norrköping, SE 601 74, Sweden

³ School of Materials Science and Engineering, Nanyang Technological University, 50 Nanyang Avenue, 639798, Singapore

⁴ State Key Laboratory of Metastable Materials Science and Technology, Yanshan University, Qinhuangdao 066004, China

* Corresponding authors: chaoyang.kuang@liu.se (C.K.), qywen@uestc.edu.cn (Q.W.), xukai@ysu.edu.cn (K.X.), and shangzhi.chen@uestc.edu.cn (S.C.)

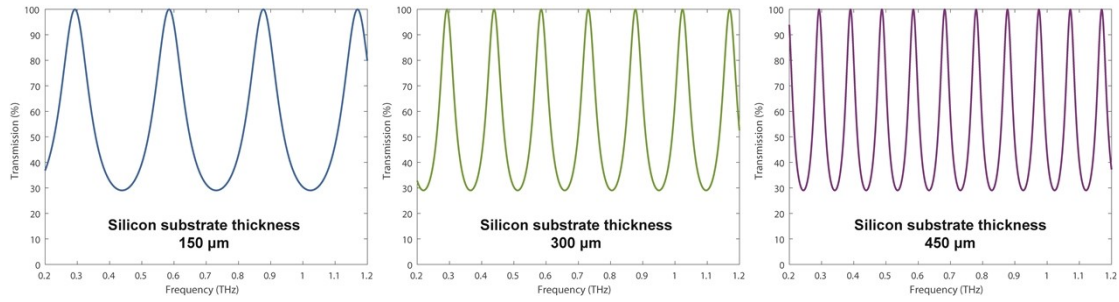


Figure S1 | The interference effect of silicon substrate in THz range.

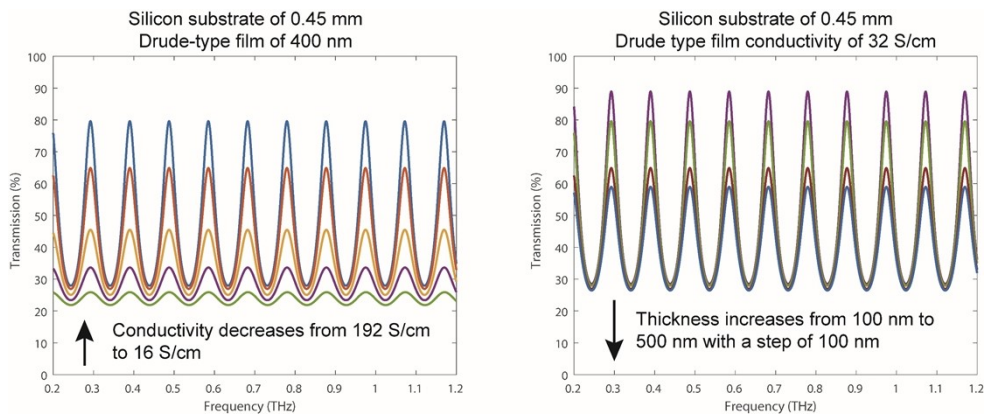


Figure S2 | The interference effect of Drude-type thin films deposited on silicon substrates.

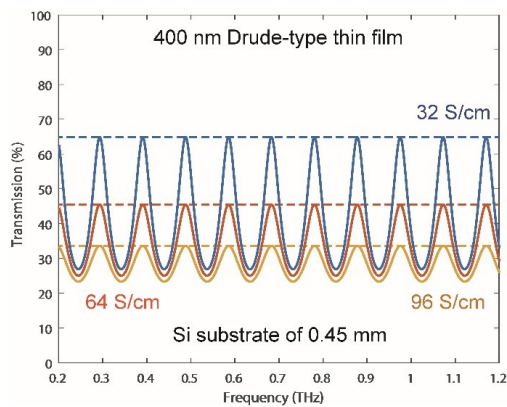


Figure S3 | The comparison of THz transmission of Drude-type thin films deposited on silicon substrates and those of free-standing Drude-type thin films.

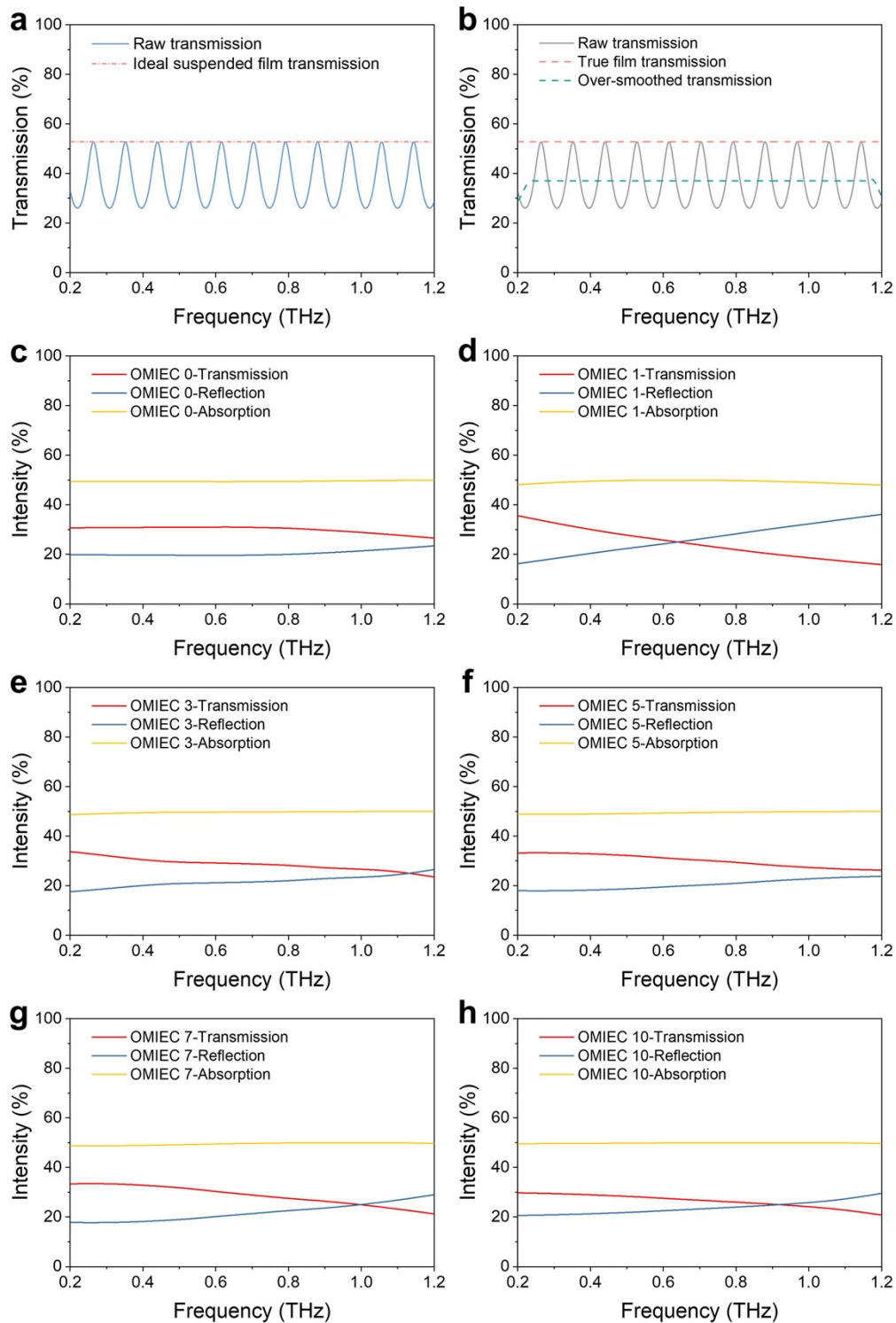


Figure S4 | THz properties of OMIEC thin films. a, The half-wave resonance matching conditions for a sample thin film deposited on a substrate. The maximum transmission of the interference oscillation corresponds to the ideal suspended thin film transmission. b, Comparison between the excessively smoothed THz curve and the film's true transmission. c-h, THz transmission, reflection and absorption curves for different OMIEC thin films.

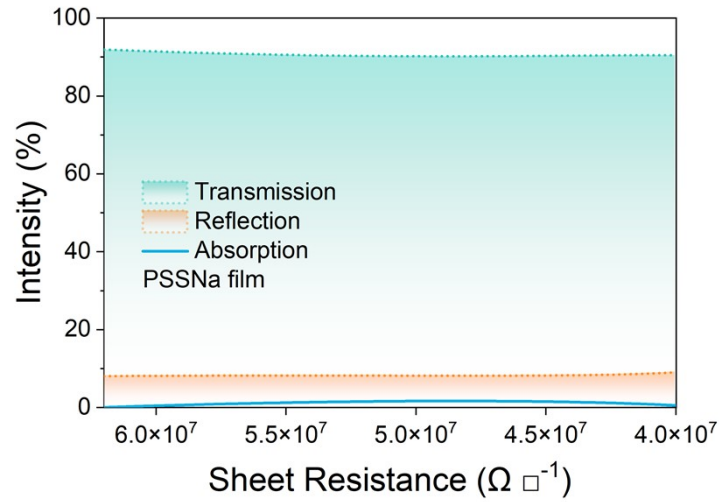


Figure S5 | THz characteristics of PSSNa thin film. Frequency-averaged THz transmission, reflection, and absorption are plotted as a function of sheet resistance. The PSSNa thin film thicknesses are ranging from 0.47 μm to 57 μm , and averaged over 0.2-1.2 THz.

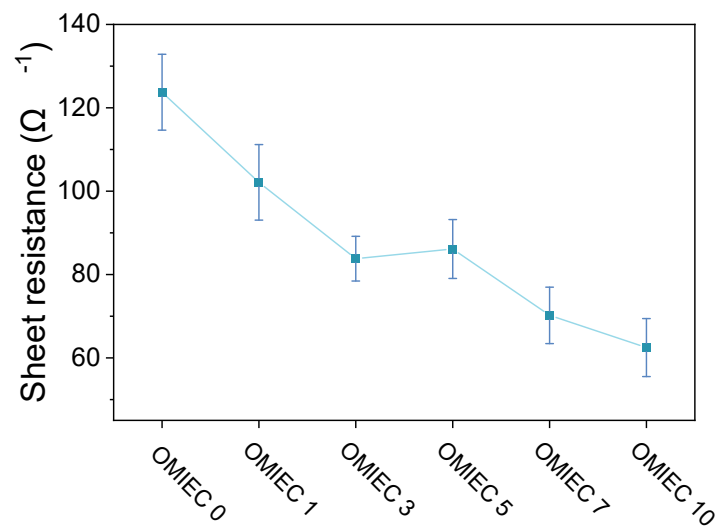


Figure S6 | Measured DC sheet resistance of OMIEC thin films.

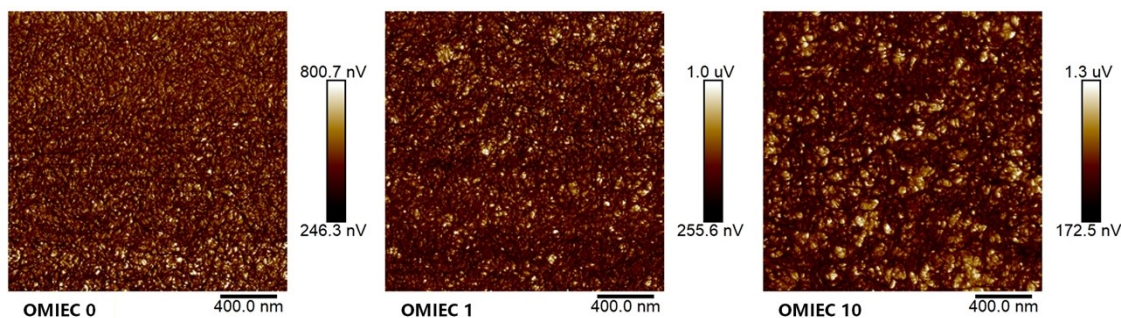


Figure S7 | AFM in-phase signal images of OMIEC thin films with varying PSSNa doping concentrations.

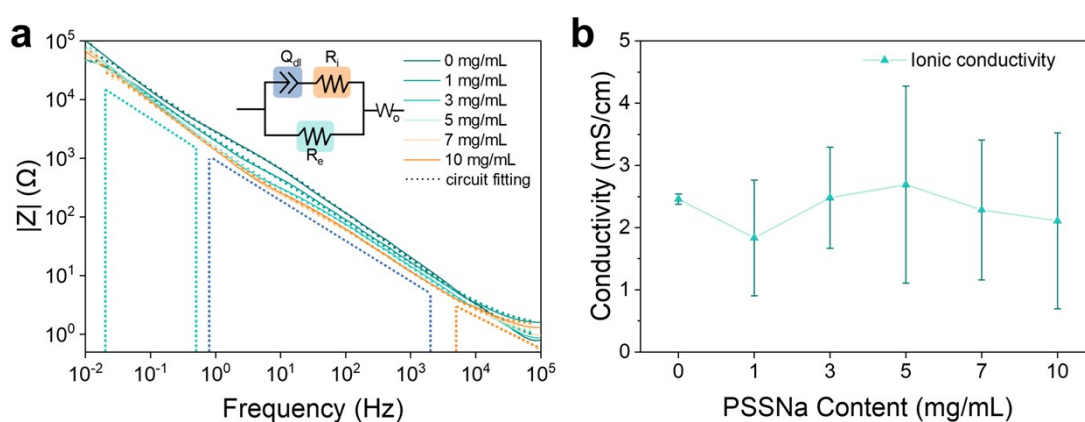


Figure S8 | EIS characterization of OMIEC thin films. (a) Bode plots ($|Z|$ versus frequency, 0.1 Hz–1 MHz). Color shading indicates dominant frequency regions: high-frequency bulk ionic pathways (orange), mid-frequency double-layer formation (blue), and low-frequency electronic pathways (green). (b) Ionic conductivity derived from equivalent circuit fitting.

The element values are extracted by equivalent circuit fitting, and the ionic conductivity in the impedance spectra is calculated using the following formula:

$$\sigma = \frac{A}{R \cdot l}$$

where A denotes the surface area of the stainless-steel electrodes, l is the electrode spacing, and R is the fitted resistance value. (Under the same THz testing conditions, 23 ± 1 °C with relative humidity below 8%.)

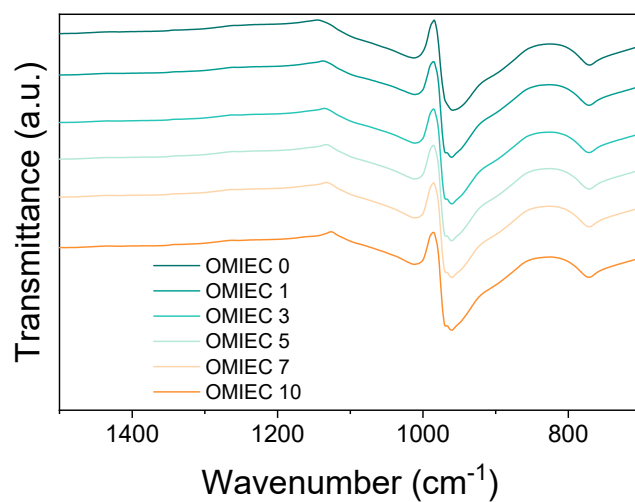


Figure S9 | ATR FT-IR spectra of OMIEC thin films with varying concentrations of PSSNa.

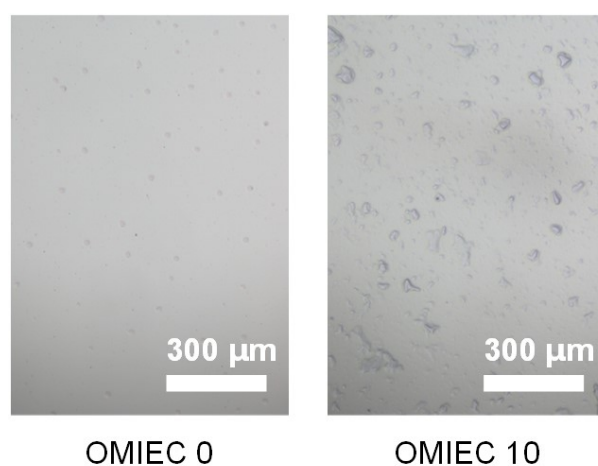


Figure S10 | Optical images of OMIEC 0 and OMIEC 10 films under a 10x optical microscope.

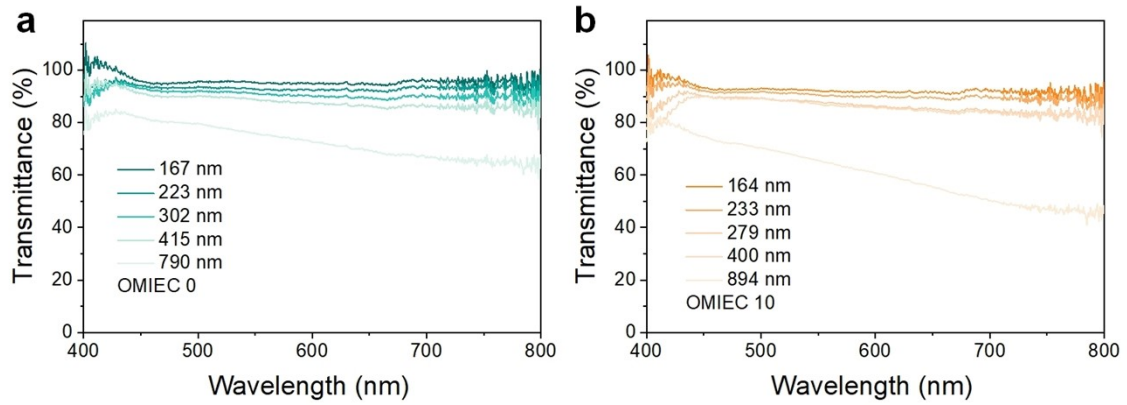


Figure S11 | Transmittance curves of OMIEC 0 and OMIEC 10 films at different thicknesses under visible light (400–800 nm).

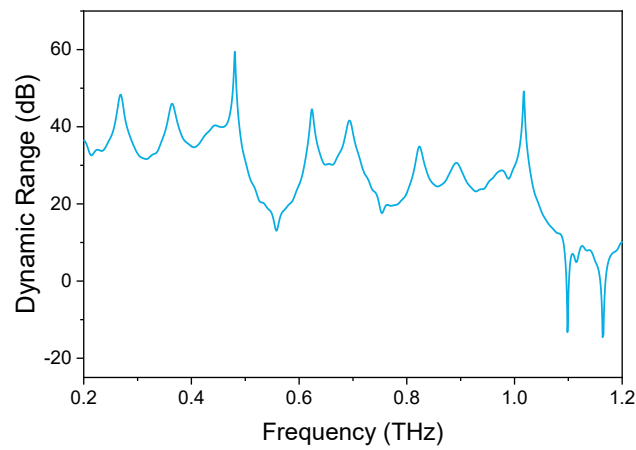


Figure S12 | Frequency-dependent dynamic range dispersion of the THz-TDS system used in this study. The dynamic range DR is defined as:

$$DR(f) = 20 \log_{10}(|E_{ref}(f)|/|E_{noise}(f)|)$$

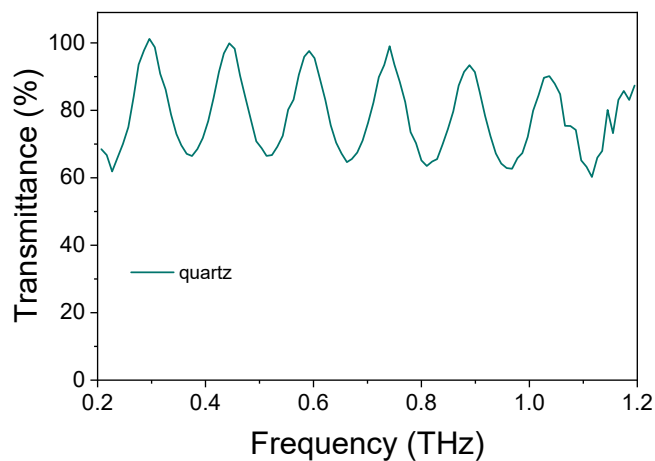


Figure S13 | Terahertz transmission curve of a blank quartz substrate.

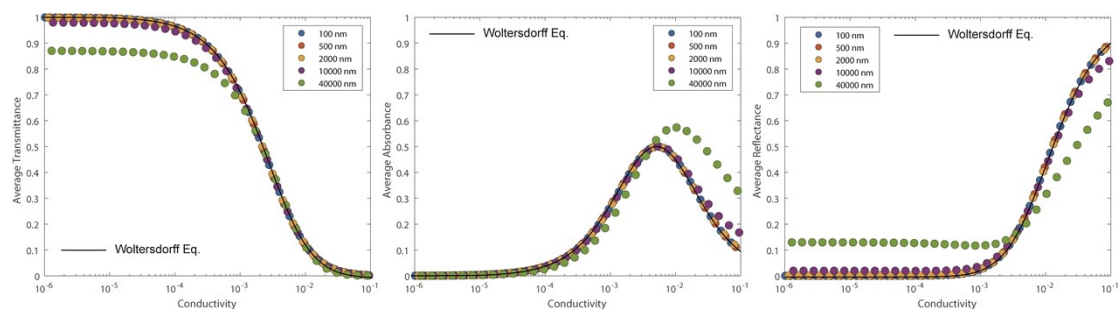


Figure S14 | The comparison of THz properties calculated by TMM and Woltersdorff equations. Thin films with different thicknesses were used.

Table S1. Thicknesses of OMIEC thin films with different PSSNa concentrations.

Sample	Thickness(nm)
OMIEC 0	415 ± 17 nm
OMIEC 1	411± 21 nm
OMIEC 3	409± 17 nm
OMIEC 5	405± 29 nm
OMIEC 7	404± 25 nm
OMIEC 10	400 ± 33 nm

Table S2 | Surface roughness of OMIEC thin films measured by AFM.

Sample	Surface roughness (nm)
OMIEC 0	5.05 nm
OMIEC 1	6.81 nm
OMIEC 10	10.78 nm

Table S3 | Extracted best-fit parameters of the complex optical conductivity dispersion of OMIEC thin films based on the simplified Drude-Debye model.

Sample name	Angular plasma frequency (rad/s)	Scattering time of Drude model (fs)	Charge carrier density (10^{21} cm^{-3})	Charge carrier mobility ($\text{cm}^2/\text{V}\cdot\text{s}$)	Effective relaxation time of Debye model (ps)
OMIEC 0	2.75	0.161	2.38	0.28	10.2
OMIEC 1	2.95	0.131	2.73	0.23	18.1
OMIEC 3	2.87	0.142	2.59	0.24	16.7
OMIEC 5	2.66	0.168	2.23	0.30	23.8
OMIEC 7	2.42	0.202	1.85	0.35	34.2
OMIEC 10	2.46	0.197	1.91	0.34	41.9

Table S4 | Chemical compositions and PSSNa doping ratios of different PEDOT:PSS samples.

Sample	GOPS (vol%)	DBSA (vol%)	PEG (vol%)	PSSNa (mg/ml)
OMIEC 0	1	0.25	5	0
OMIEC 1	1	0.25	5	1
OMIEC 3	1	0.25	5	3
OMIEC 5	1	0.25	5	5
OMIEC 7	1	0.25	5	7
OMIEC 10	1	0.25	5	10

Table S5 | Data for OMIEC 0 and OMIEC 10 samples of different thicknesses in **Figure 2e**.

OMIEC 0 (nm)	OMIEC 10 (nm)
167 ± 7 nm	164 ± 23 nm
223 ± 12 nm	233 ± 33 nm
303 ± 15 nm	279 ± 24 nm
415 ± 17 nm	400 ± 33 nm
790 ± 23 nm	894 ± 34 nm